olefin hydrogenation,[22] rapid insertion would imply an ability of the $H_2Fe(CO)_3C_2H_4$ complex to adopt a *cis*-hydrido–ethylene configuration with parallel Fe—H and $CH_2$=$CH_2$ bonds, a not unreasonable proposition, for facile formation of a four-center transition state.

An alternative mechanism, which we present in the light of new information on dihydrogen–metal interactions,[23] is that hydrogen binds to $Fe(CO)_3C_2H_4$ to form, not a dihydride, but a dihydrogen ($\eta^2$-$H_2$) molecular complex. Such complexes, of which many examples have been found since their discovery in 1983, have recently been proposed as intermediates in the photocatalytic hydrogenation of norbornadiene.[24] In the case of $Fe(CO)_3(C_2H_4)$, $H_2$ approaching from either side of the square-planar structure will form $Fe(CO)_3(C_2H_4)(H_2)$ in a configuration set up so that hydrogen transfer can take place through a five-center transition state in which the radical center, formed as the Fe transfers to the opposite ethylene carbon, essentially abstracts a hydrogen atom from the $\eta^2$-bound $H_2$ molecule.

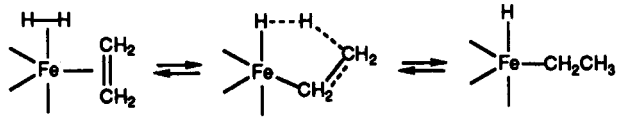


Hydrogen scrambling would again take place through the reversiblity of this reaction and rotation of ethylene in the dihydrogen–ethylene complex. Under rapid equilibrium, a value of $R = 1.5$ would also be expected from this mechanism. Both dihydrido and dihydrogen mechanisms require relatively facile rotation of the ethylene about its $\eta^2$ bond. Factors affecting the barrier to this type of motion, which for some configurations could be prohibitively high, have been discussed by Albright et al.[25] However, knowledge of the structure of either the dihydrido or the dihydrogen complex is insufficient to distinguish their roles by analogy to structures where ethylene rotation has been studied.

## Conclusion

$Fe(CO)_3$-mediated hydrogenation of ethylene using hydrogen/deuterium mixtures results in deuterium distributions in the ethane product which support the concept that the hydrogenation reaction takes place as an intramolecular rearrangement of an iron complex containing both reactants to form an alkyl hydrido complex, followed by alkane elimination. The statistical distribution between *1,1-*$d_2$ and *1,2-*$d_2$ ethane products demonstrates that rapid hydrogen atom migration can take place in this process, suggesting that the step involving hydrogen insertion into ethylene is reversible. At present, it is not possible to distinguish the form of the hydrogen complex that accommodates this insertion: it may be either a classic dihydrido complex or a molecular dihydrogen complex.

(22) Thorn, D. L.; Hoffmann, R. *J. Am. Chem. Soc.* **1978**, *100*, 2079.
(23) Kubas, G. J. *Acc. Chem. Res.* **1988**, *21*, 120.
(24) Jackson, S. A.; Hodges, P. M.; Poliakoff, M.; Turner, J. J.; Grevels, F.-W. *J. Am. Chem. Soc.* **1990**, *112*, 1221.
(25) Albright, T. A.; Hoffmann, R.; Thibeault, J. C.; Thorn, D. L. *J. Am. Chem. Soc.* **1979**, *101*, 3801.

# Electron-Transfer Equilibria and Kinetics of *N*-Alkylphenothiazines in Micellar Systems

**Ezio Pelizzetti,* Emilia Fisicaro,**

*Istituto di Chimica Fisica Applicata, Università di Parma, 43100 Parma, Italy*

**Claudio Minero, Alberto Sassi,**

*Dipartimento di Chimica Analitica, Università di Torino, 10125 Torino, Italy*

**and Hisao Hidaka**

*Department of Chemistry, Meisei University, Hodokubo, Hino-shi Tokyo 191, Japan* *(Received: May 8, 1990; In Final Form: July 16, 1990)*

The kinetics and equilibria of electron transfer between *N*-alkylphenothiazines (alkyl = methyl, ethyl, butyl, dodecyl) and aquoiron(III)/(II) in the presence of various micellar forming surfactants (hexadecyltrimethylammonium methanesulfonate, sodium dodecylsulfate, and Triton X100) were investigated. The presence of the micelles strongly affects rates and equilibria, and the dependence of these changes on the hydrophobicity of the alkyl chain is examined.

## Introduction

Micelles are dynamic aggregates of amphiphilic molecules and possess regions of hydrophilic and hydrophobic character. They are often used as models systems to mimic cellular membranes[1] because the variety of interactions that may be operative between solubilized substrates and host structures, including electrostatic attraction, pseudophase extraction, and surface adsorption.

Work in these laboratories has addressed the effects of micellar systems on the redox equilibria and reactivities of solubilized organic substrates with metal ion complexes.[2,3]

*N*-Alkylphenothiazine derivatives represent an interesting and versatile class of compounds. In addition to their importance in the physiological activity,[4] these compounds exhibit important photoredox properties[5] and are suitable compounds for the investigation of organic radicals because of the easy formation of

**CHART I: Chemical Structure, Chemical Name, and Symbols for *N*-Alkylphenothiazines Derivatives Used in the Work**

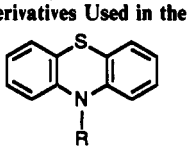


| chemical name | R | symbol |
|---|---|---|
| phenothiazine | H | $C_0$PTZ |
| *N*-methylphenothiazine | $CH_3$ | $C_1$PTZ |
| *N*-ethylphenothiazine | $C_2H_5$ | $C_2$PTZ |
| *N*-butylphenothiazine | $C_4H_9$ | $C_4$PTZ |
| *N*-dodecylphenothiazine | $C_{12}H_{25}$ | $C_{12}$PTZ |

* To whom correspondence should be addressed.

0022-3654/91/2095-0761$02.50/0 

stable cation radicals by removal of one electron from the parent molecule.[6]

The combination of kinetic and equilibria measurements on the one-electron-transfer equilibrium and kinetics between a series of *N*-alkylphenothiazines (see Chart I) and iron(III)/(II) couple will allow the estimation of the electrostatic and hydrophobic contribution to the interactions of charged species with micellar aggregates.

## Experimental Section

*Reagents.* $C_1PTZ$ was supplied by Aldrich and recrystallized from Ar-saturated ethanol. The other $C_nPTZ$'s ($n$ = 2, 4, 12) were prepared by literature procedures.[7] Stock solutions of iron(II) were prepared by dissolution of metal iron (Aldrich, >99.99%) in $HClO_4$ (Merck, PA grade) and standardized by oxidimetric titration. Iron(III) stock solution was prepared by electroxidation of the iron(II) solution and standardized through complexometric titration.

The surfactants sodium dodecylsulfate (SDS, Fluka) and hexadecyltrimethylammonium bromide (CTAB, Aldrich) were recrystallized before use. Hexadecyltrimethylammonium methanesulfonate (CTAS) was prepared by neutralization with methanesulfonic acid (Aldrich) of hexadecyltrimethylammonium hydroxide (CTAOH) obtained by ionic exchange of CTAB over Amberlite CG-400 resin, Fluka. Methanesulfonic acid was standardized through alkalimetric titration, and sodium methanesulfonate was prepared by the neutralization of the acid with NaOH. Triton X-100 (Aldrich) and octaethyleneglycol dodecyl ether ($C_{12}E_8$) were used as supplied.

All measurements were carried out with $NaClO_4$ as excess salt, except when CTAS was used and an excess sodium methanesulfonate was utilized.

*Spectroscopic Measurements.* UV–visible spectra were measured by using a Varian Cary 219 spectrophotometer. The molar absorptivities were verified by oxidizing the phenothiazines with hexachloroiridate(IV), an oxidant that ensures the complete oxidation of $C_nPTZ$. The wavelength region around 520 nm proved particularly useful for following the course of the reaction because only the cation radicals have significant molar absorptivities.

*Kinetics.* A Hitech stopped-flow spectrophotometer with 1-cm cell path was employed for reactions of $C_nPTZ$ with Fe(III)/(II). The measurements were performed at $[C_nPTZ] = 1 \times 10^{-5}$ M, while the concentrations of Fe(III)/(II) were dependent on the surfactant system. The following experimental conditions were employed: $[CH_3SO_3H] = 0.01$ M and $\mu = 0.10$ M ($CH_3SO_3Na$).

All kinetic experiments were performed at 25.0 ± 0.1 °C. When possible, the concentration of reactants for reaction 1, from

$$C_nPTZ + Fe(III) \underset{k_{-1}}{\overset{k_1}{\rightleftharpoons}} C_nPTZ^{\bullet+} + Fe(II) \qquad (1)$$

$$-d[C_nPTZ]/dt = k_1[Fe(III)][C_nPTZ] - k_{-1}[Fe(II)][C_nPTZ^{\bullet+}] \qquad (2)$$

which rate law 2 results, were chosen to ensure pseudo-first-order conditions; that is, both Fe(III) and Fe(II) were added in relatively high concentrations with respect to $C_nPTZ$. Under these conditions plots of ln $(A_\infty - A_t)$ vs time (where $A_\infty$ and $A_t$ represent the absorbance at equilibrium and at time $t$, respectively) were linear for at least 90% of the reaction. The slopes of the plots define pseudo-first-order rate constants for the approach to equilibrium (see eq 3). To evaluate the specific rate constants, $k_{obs}/[Fe(II)]$ was plotted against the [Fe(III)]/[Fe(II)] ratio.

$$k_{obs} = k_1[Fe(III)] + k_{-1}[Fe(II)] \qquad (3)$$

In the case where comparable concentrations were used or both products of reaction are initially absent (e.g., reduction of $C_nPTZ^{\bullet+}$ with Fe(II)), the proper kinetic equations were adopted to obtain the specific rate constants.[8] The standard deviations of each of the rate constants were in the range 3–5%.

*Micellar Binding Constants.* These parameters were derived from equilibrium or kinetic data obtained at different micellized surfactant concentrations (see below). Comparison with previous data obtained in different experimental conditions is reported in Table II.

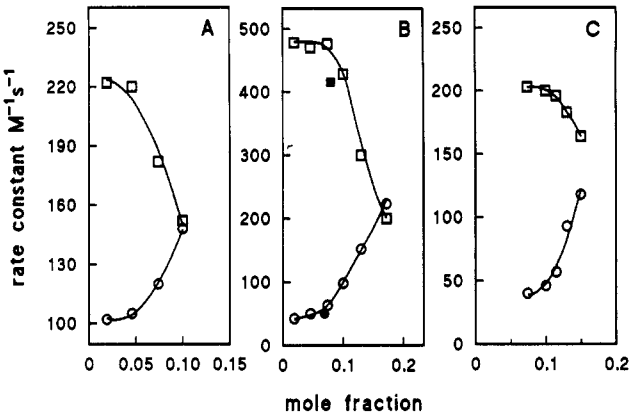


**Figure 1.** Rate constants for forward (□) and backward (○) reactions of eq 1 as a function of the mole fraction of methanol. Closed symbols for ethanol. A, $C_1PTZ$; B, $C_2PTZ$; C, $C_4PTZ$.

**TABLE I: Values Adopted in Eq 1 as Specific Rate Constants in Aqueous Media for Different $C_nPTZ$'s[a]**

| compd | $k^w_1$, $M^{-1}$ $s^{-1}$ | $k^w_{-1}$, $M^{-1}$ $s^{-1}$ | $K^w_1$ |
|---|---|---|---|
| $C_1PTZ$ | 230 | 100 | 2.3 |
| $C_2PTZ$ | 480 | 40 | 12 |
| $C_4PTZ$ | 210 | 33 | 6.5 |

[a] The kinetic values are weighted averages over different observations (see text). The estimated standard deviations are ca. 10–15%. The corresponding equilibrium constants have a confidence of ca. 20–25%.

## Results

*Equilibria and Kinetics in the Absence of Surfactants.* Because of the importance in the following discussion section of the kinetic and equilibrium data in aqueous solution, several attempts were carried out to obtain reliable estimates of these values. The difficulties arise from the low solubility of $C_nPTZ$'s, which obviously becomes lower as the alkyl chain length $R$ increases. Thus, whereas for $C_1PTZ$ measurements performed at 5 and 10% v/v of methanol and 20% of ethanol show that $k_1$ and $k_{-1}$ are very little affected by organic solvent content in the considered range, and the values 230 and 100 $M^{-1}$ $s^{-1}$, respectively, can be extrapolated safely as the corresponding aqueous values (see Figure 1A); the same procedure is less straightforward for $C_2PTZ$ and $C_4PTZ$, while it is not possible for $C_{12}PTZ$ due to the possibility of solubilization only at high percentage of organic solvent.

In the case of $C_2PTZ$ and $C_4PTZ$, the influence of solvent composition becomes already evident at low organic solvent content, due to the increasing hydrophobicity and to the higher stabilizing/destabilizing effect of solvent composition on initial reagent/products and the activated states.[9]

(1) Fendler, J. H. *Membrane Mimetic Chemistry*; Wiley: New York, 1982.
(2) Minero, C.; Pramauro, E.; Pelizzetti, E.; Meisel, D. *J. Phys. Chem.* **1983**, *87*, 399.
(3) Pramauro, E.; Pelizzetti, E. *J. Phys. Chem.* **1984**, *88*, 990.
(4) Forrest, I. S., Carr, C. J., Usdin, E., Eds. *Adv. Biochem. Psychopharmacol.* **1974**, *9*.
(5) Infelta, P. P.; Graetzel, M.; Fendler, J. H. *J. Am. Chem. Soc.* **1980**, *102*, 1479.
(6) Pelizzetti, E.; Mentasti, E. *Inorg. Chem.* **1979**, *18*, 583.
(7) (a) Bernthsen, A. *Liebigs Ann. Chem.* **1885**, *230*, 73. (b) Normant, H.; Curigny, T. *Boll. Soc. Chim. Fr.* **1965**, 1866. (c) Humphrey-Baker, R.; Braun, A. M.; Graetzel, M. *Helv. Chim. Acta* **1981**, *64*, 2036.
(8) Frost, A. A.; Pearson, R. G. *Kinetics and Mechanisms*; Wiley: New York, 1961.

SCHEME I

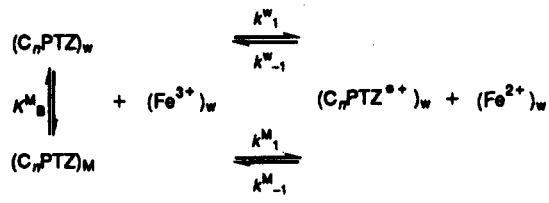


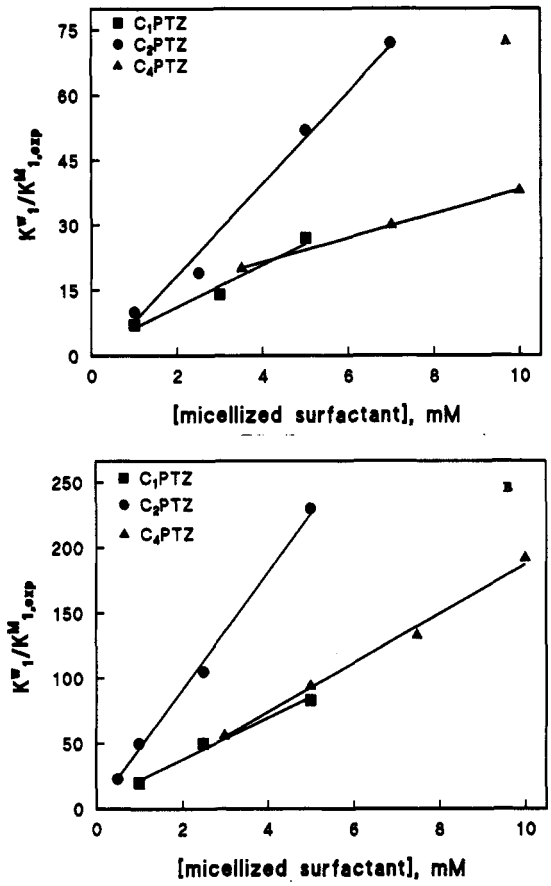


Figure 2. Plots for eq 1, according to eq 4, in the presence of Triton (left) and CTAS (right). For $C_4PTZ$ abscissa scale ×10.

From Figure 1B,C it is evident that the more difficult data to extrapolate refer to the reverse reaction in eq 1. Then, kinetic measurements on the reaction between $C_2PTZ^{\bullet+}$ and $C_4PTZ^{\bullet+}$ electrochemically generated with Fe(II) have been carried out with a limited amount of methanol in solution (less or equal to 8% v/v).

Averaged measurements gave 40 ± 5 and 37 ± 6 $M^{-1}$ $s^{-1}$ for the rate constant of the reverse reaction 1 of $C_2PTZ$ and $C_4PTZ$, respectively. These values compare also well with the data derived for the reverse reaction in the presence of CTAS and Triton (see below).

In conclusion, the values reported in Table I were adopted for $k^w_1$ and $k^w_{-1}$ [$M^{-1}$ $s^{-1}$], and for the equilibrium constants in water $K^w_1$ for the different $C_nPTZ$'s.

*Kinetic Data and Equilibria in the Presence of Micelles.* The specific rate constants and equilibrium data in the presence of CTAS, Triton and SDS are presented in Figures 2, 3, 5, and 6.

## Discussion

*Equilibria and Kinetics in the Presence of Cationic and Nonionic Micelles.* As far as equilibrium and kinetics of $C_1PTZ$, $C_2PTZ$, and $C_4PTZ$ with the Fe(III)/Fe(II) couple are concerned, the changes as a function of CTAS and Triton concentration are as expected for a situation where $Fe^{3+}$, $Fe^{2+}$, and $C_nPTZ^{\bullet+}$ are

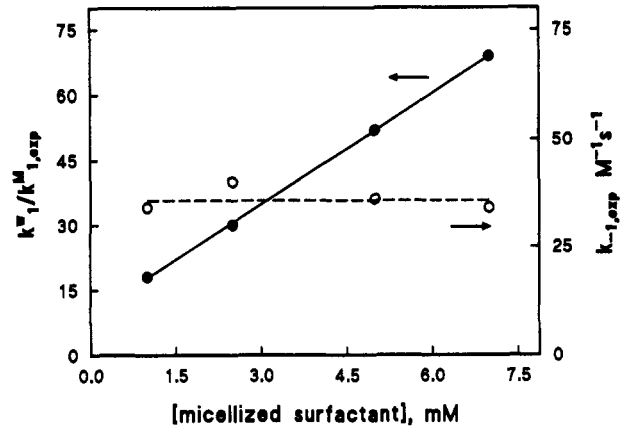


Figure 3. Rate constants for $C_2PTZ$ in the presence of Triton. Closed circles, plot according to eq 6 for the forward reaction (left scale); open symbols, backward reaction (right scale).

TABLE II: Values of Binding Constants $K^M_B$ ($M^{-1}$)

| compd | CTA | Triton | ref |
|---|---|---|---|
| $C_0PTZ$ | $3 \times 10^4$ [a] | $3 \times 10^3$ [a] | 10 |
| $C_1PTZ$ | $2.5 \times 10^4$ [b] | $6.4 \times 10^3$ [c] | 2 |
| | $1.6 \times 10^4$ [d] | $5.5 \times 10^3$ [d] | e |
| $C_2PTZ$ | $4.2 \times 10^4$ [d] | $1.0 \times 10^4$ [d] | e |
| $C_4PTZ$ | $1.9 \times 10^4$ [d] | $3.5 \times 10^4$ [d] | e |

[a] 0.50 M $NO_3^-$. [b] 0.10 M $NO_3^-$. [c] 0.10 M $ClO_4^-$. [d] 0.10 M $CH_3SO_3^-$. [e] This work.

almost entirely in the aqueous phase and $C_nPTZ$'s are partially bound to the micelles (Scheme I).

The observed equilibrium constant in the presence of micelles, $K^M_{1,exp}$, is then related to the equilibrium constant in the absence of surfactant, $K^w_1$, through eq 4, where $K^M_B$ represents the association constant for $C_nPTZ$ with CTAS and Triton and [D] is the concentration of surfactant that exceeds the critical micelle concentration (cmc). The value of the association constant is obtained by plotting $K^w_1/K^M_{1,exp}$ as a function of [D]. Figure 2 parts A and B, show the data for $C_nPTZ$ ($n$ = 1, 2, 4) in Triton and CTAS, respectively.

$$K^M_{1,exp} = \frac{K^w_1}{1 + K^M_B[D]} \quad (4)$$

Kinetic data can similarly be analyzed in the framework of Scheme I. In fact $k_{-1,exp}$ is essentially independent for all the investigated systems ($C_1PTZ$, $C_2PTZ$, $C_4PTZ$) of the surfactant concentration (either CTAS or Triton), whereas the observed $k_{1,exp}$ decreases with the increasing of [D].

Since it was shown that the rate of entrance and exit of solubilizates in and out of the micelle occurs in the microsecond time scale, it is clear that the $C_nPTZ$ equilibrium between the aqueous and micellar subphases is achieved much faster than the rate of approach to equilibrium of reaction 1. This model leads to the following equation for the total forward reaction:

$$k^M_{1,exp} = \frac{k^w_1 + k^M_1 K^M_B[D]}{1 + K^M_B[D]} \quad (5)$$

where $k^w_1$ and $k^M_1$ represent the rate constants in the aqueous and cationic or nonionic micellar pseudophase, respectively.

It has been shown in the case of $C_0PTZ$[10] and $C_1PTZ$[2] that the contribution of the reaction progress in the micellar pseudophase can be neglected; then eq 5 can be rewritten as

$$\frac{1}{k^M_{1,exp}} = \frac{1}{k^w_1} + \frac{K^M_B}{k^w_1}[D] \quad (6)$$

(9) (a) Burgess, J.; Pelizzetti, E. *Gazz. Chim. Ital.* **1988**, *118*, 803. (b) Blandamer, M. J.; Burgess, J. *Pure Appl. Chem.* **1982**, *54*, 2285.

(10) Pelizzetti, E.; Pramauro, E. *Ber. Bunsen-Ges. Phys. Chem.* **1979**, *83*, 996.

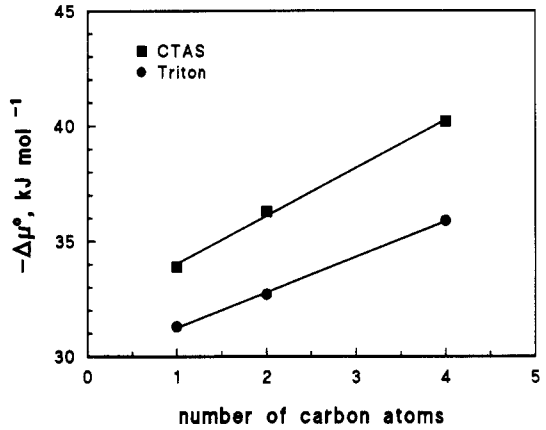


**Figure 4.** Free energy of transfer from water to micellar pseudophase, defined as in eq 7, for $C_nPTZ$'s as a function of the number of carbon atoms of the alkyl chain.

Plots according to eq 6 are reported in Figure 3. The values of $K^M_B$ thus derived are close to those evaluated from the plots such as in Figure 2.

The values of the binding constants of $C_nPTZ$ with CTAS and Triton are collected in Table II for the investigated systems together with literature references.

The transfer free energy per mole of a solute from water to the micellar pseudophase is related to $K^M_B$ by[3]

$$\Delta\mu^0 = \mu_M{}^0 - \mu_w{}^0 = -RT \ln (55.5K^M_B) \quad (7)$$

Since the micellar incorporation in the present systems is primarily determined by hydrophobic interactions, the free energy change can be tentatively expressed as the sum of two contributions, one arising from the aromatic residue and one from the alkyl substituent:

$$\Delta\mu^0 = \mu_M{}^0 - \mu_w{}^0 = \mu_{PTZ}{}^0 + n\mu_c{}^0 \quad (8)$$

where $n$ is the number of aliphatic carbon atoms.

Figure 4 shows the variations of the transfer free energy calculated from eq 7 as a function of the number of aliphatic carbons of the substituent $R$. The slope corresponds to the contribution of each aliphatic carbon atom to the transfer free energy. The difference observed in the binding between CTAS and Triton for the same compound can be explained by the interaction of the aromatic moiety with the positive charge of the CTAS micelle. The contribution of the aliphatic carbon is however comparable (2.2 kJ mol$^{-1}$ for CTAS and 1.6 kJ mol$^{-1}$ for Triton), and it is less than what has been observed for alkanes. In addition, if the data are compared to values obtained for the free energy of micellization for a variety of surfactants (ca. 3 kJ mol$^{-1}$ per $CH_2$ group), it can be inferred that the solubilization of $C_nPTZ$'s ($n$ = 0, 1, 2, 4) takes place in a more hydrated region than the core of the micelle. For the series $C_nPTZ$ ($n$ = 0, 1, 2) the solubilization in SDS allowed an estimate of ca. 1.5–1.9 kJ mol$^{-1}$ per $CH_2$ group.[11]

Runs starting with electrochemically generated $C_4PTZ^{\bullet+}$ reacting with Fe(II) in the presence of 0.05–0.10 M CTAS (in the presence of 5% v/v methanol) or the presence of 0.01 M $C_{12}E_8$ gave rate constants of the order of 0.35 ± 0.05 M$^{-1}$ s$^{-1}$ independent of the surfactant concentration.

These results are evidence that the association constants for $C_4PTZ^{\bullet+}$ are ≤2 and ≤20 M$^{-1}$ for CTAS and $C_{12}E_8$, respectively. Then the interaction between the radical cation in the CTAS micelles is due not merely to electrostatic repulsion but to hydrophilic effect arising from the preference of the radical cation for the water environment rather than the less polar micellar pseudophase.

Similar dramatic changes in the hydrophilicity have been noted for *N*-dodecyl-*N'*-methyl-4,4'-dipyridinium chloride system (dodecylviologen, $C_{12}MV^{2+/+}$ couple). In fact $C_{12}MV^{2+}$ is also so hydrophilic that it is present only in water even in CTAB solutions, whereas $C_{12}MV^+$ exhibits a strong tendency to associate with cationic aggregates.[12]

Another example is represented by the behavior of (ferrocenylmethyl)dodecyldimethylammonium bromide, which in the reduced state (+1 charge) forms micelles that are broken into monomers when the surfactant is in the oxidized state (+2 charge). This can be attributed to the enhancement in the electrostatic repulsion among positively charged head groups and their increasing hydrophilic character as well.[13]

As noted above, the lack of interaction of $C_nPTZ^{\bullet+}$ with nonionic aggregates is slightly more surprising. Interactions of other positively charged species with Triton micelles has been reported. This is the case of some $CoL_3{}^{2+}$ and $RuL_3{}^{2+}$ complexes (where L is a bipyridine- or phenanthroline-like ligand) that associate with nonionic micelles, whereas the oxidized species (+3 charge) do not.[14-16]

These examples reveal that owing to the competition between water molecules and micellar aggregates, the balance between hydrophilic and hydrophobic effects is extremely delicate for the association with uncharged micelles.

Finally it is worth noting that the reaction rate between $Fe^{3+}$ and $C_nPTZ$'s embedded in CTAS aggregates is decreased by more than 3 orders of magnitude. This can be attributed to the electrostatic repulsion between $Fe^{3+}$ and the positive charge of the micelle. On the basis of the probability of encounter between $CTA^+$ micelle and the iron species, simply expressed by the Boltzmann term (see below), at 0.01 M ionic strength (the present condition) a value of ca. $10^{-4}$ can be derived.[17]

Electrostatic repulsion cannot be invoked in the case of nonionic micelle, but again the reaction rate is reduced by at least 2 orders of magnitude. This observation could be attributed to the location of aromatic moiety of $C_nPTZ$ in a less accessible region and seems to be confirmed by the lack of appreciable reaction of $C_{12}PTZ$ in nonionic micelles.

A recent work pointed out that the photoionization yield of sulfonated alkylphenothiazines in vesicles increased with a decrease in the alkyl chain length (from 3 to 6 and 12 carbon atom chains), and this fact was explained by a model in which the $C_nPTZ$'s are located deeper into the vesicle the longer the alkyl chain.[18] This can be even more important in the present case where no hydrophilic groups, such as sulfonic, are present in the molecule.

*Equilibria and Kinetics in Anionic Micelles.* Equilibrium 1 was investigated also in anionic micelles of SDS. Kinetic data were collected for $C_2PTZ$, $C_4PTZ$, and $C_{12}PTZ$ (in $CH_3SO_3Na$ medium). Plots of $r_1$ ($k_{1,exp}/k^w_1$) and $r_{-1}$ ($k_{-1,exp}/k^w_{-1}$) are depicted in Figure 5. Below $5 \times 10^{-3}$ M SDS solubility problems arise; then the characteristic bell-shaped curves observed when both reactants interact with the micellar pseudophase (see for example $C_1PTZ^2$) are represented here only by the decreasing part after the maximum has been reached (located at ca. $3 \times 10^{-3}$ M SDS for $C_1PTZ$). Lines are drawn only for similarity with $C_1PTZ$ behavior.

Some interesting features are emerging from the observation of Figure 5: (a) For all $C_nPTZ$'s, $r_{-1}$ is always bigger than $r_1$, contrary to the expectation based solely on electrostatic considerations for $Fe^{3+}$ vs $Fe^{2+}$ ions. (b) If the electrostatic enrichment in the Stern layer of the micellar–water interface is calculated according to a computational model that was found to be satisfactory in other systems,[19] the forward reaction rate increase can largely be attributed to the increased local concentration of $Fe^{3+}$

(11) Moroi, Y.; Noma, H.; Matuura, R. *J. Phys. Chem.* **1983**, *87*, 872.

(12) Brugger, P. A.; Infelta, P. P.; Braun, A. M.; Graetzel, M. *J. Am. Chem. Soc.* **1981**, *103*, 320.

(13) Saji, T.; Hoshino, K.; Aoyagui, S. *J. Am. Chem. Soc.* **1985**, *107*, 686.

(14) Carbone, A. I.; Cavasino, F. P.; Sbriziolo, C.; Pelizzetti, E. *J. Phys. Chem.* **1985**, *89*, 3578.

(15) Hauenstein, Jr., B. L.; Dressick, W. J.; Gilbert, T. B.; Demas, J. N.; DeGraaf, B. A. *J. Phys. Chem.* **1984**, *88*, 1902.

(16) Dressick, W. J.; Hauenstein, Jr., B. L.; Gilbert, T. B.; Demas, J. N.; DeGraaf, B. A. *J. Phys. Chem.* **1984**, *88*, 3337.

(17) Fernandez, M. S.; Fromherz, P. *J. Phys. Chem.* **1977**, *81*, 1755.

(18) Sakaguchi, M.; Hu, M.; Kevan, L. *J. Phys. Chem.* **1990**, *94*, 870.

(19) Frahm, J.; Dieckmann, S. *J. Colloid Interface Sci.* **1979**, *70*, 440.

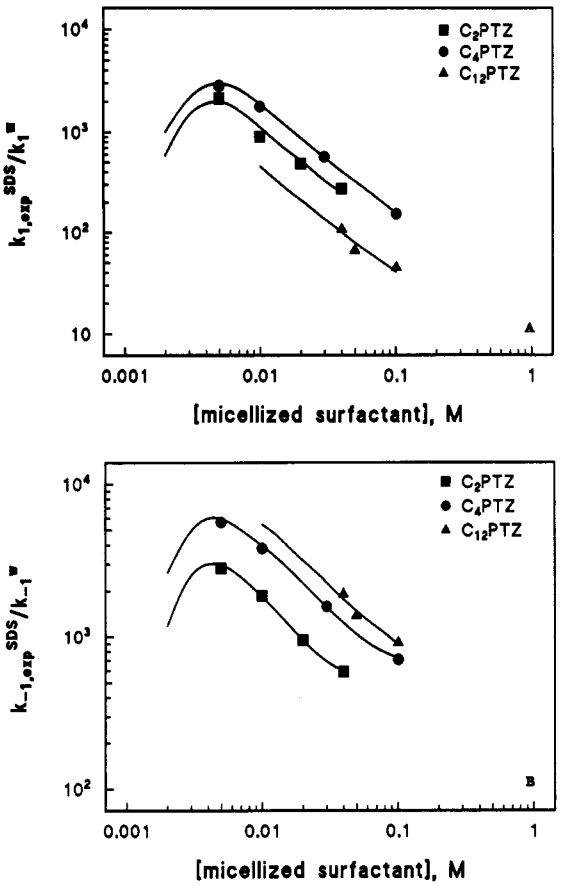


**Figure 5.** Ratio of forward reaction rates (left) and of backward reaction rates (right) in SDS and in water for $C_nPTZ$'s as a function of the surfactant concentration.

**SCHEME II**

$$\begin{array}{ccccc} (C_nPTZ)_w & + & (Fe^{3+})_w & \underset{k^w_{-1}}{\overset{k^w_1}{\rightleftharpoons}} & (C_nPTZ^{\bullet+})_w + (Fe^{2+})_w \\ \Big\downarrow K^{SDS}_B & & \Big\downarrow K^{SDS}_{Fe(III)} & & \Big\downarrow K^{SDS}_{B^+} \quad \Big\downarrow K^{SDS}_{Fe(II)} \\ (C_nPTZ)_M & + & (Fe^{3+})_M & \underset{k^M_{-1}}{\overset{k^M_1}{\rightleftharpoons}} & (C_nPTZ^{\bullet+})_M + (Fe^{2+})_M \end{array}$$

for $C_2PTZ$ and $C_4PTZ$ systems (note that this last shows a slightly higher increase).

In the case of the backward reaction, after the electrostatic enrichment for $Fe^{2+}$ is taken into account, a remaining factor ranging from ca. 25 for $C_1PTZ$ up to 80 for $C_4PTZ$ can be calculated. A possible explanation could be the increase of the electron-transfer rate in the less polar micellar interface, due for example to the stabilization of the intermediates and the products of reaction. In this respect it is worth noting that as shown in Figure 1, the forward reaction rates decrease by ca. a factor of 1.5–2 in going from water to aqueous 30% v/v methanol, whereas increasing factors around 1.5 for $C_1PTZ$ and of 4–5 for $C_2PTZ$ and $C_4PTZ$ are observed in the same range of solvent composition. Also $r_1$ could be higher than expected only on an electrostatic basis if the decrease of equilibrium quotient and the solvent effect (a decreasing behavior in this case can be noted from Figure 1) are accounted for. In this case an increase of the rate constant of electron self-exchange for $C_nPTZ^{\bullet+}/C_nPTZ$ couple could be also responsible for the experimental observations.[20,21]

For $C_{12}PTZ$ the points in Figure 5 are derived under the assumption that $k^w_1$ and $k^{w-1}$ are identical with those for $C_4PTZ$. Whereas $r_{-1}$ follows the trend, $r_1$ lies below the corresponding points reported for $C_1PTZ$–$C_4PTZ$. A different location of the

(20) Kowert, B. A.; Marcoux, L.; Bard, A. J. *J. Am. Chem. Soc.* **1972**, *94*, 5538.

(21) Sorensen, S. P.; Bruning, W. H. *J. Am. Chem. Soc.* **1973**, *95*, 2445.

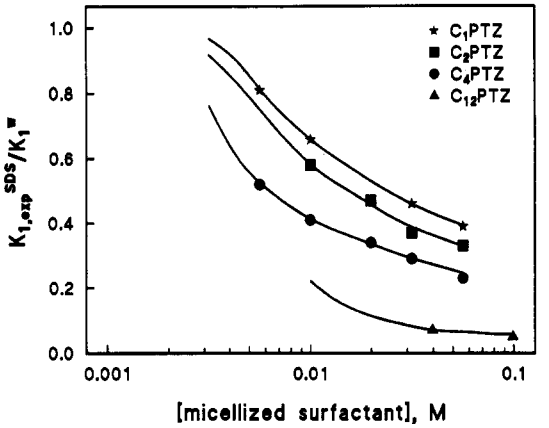


**Figure 6.** Ratio of equilibrium constants in SDS and in water for $C_nPTZ$'s as a function of the surfactant concentration; $K_1^w$ for $C_{12}PTZ$ has been assumed to be the same as for $C_4PTZ$.

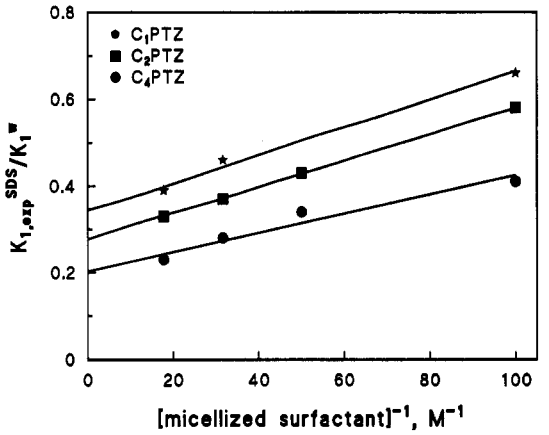


**Figure 7.** Plots according to eq 11 of the ratio of equilibrium constants in SDS and in water for $C_nPTZ$'s as a function of the reciprocal surfactant concentration.

highly hydrophobic $C_{12}PTZ$ in the micellar aggregate in respect to the radical cation could explain this observation.

The analysis of the behavior of the equilibrium data can be carried out on the basis of Scheme II. From Scheme II eq 9 is

$$K^{SDS}_{1,exp} = K^w_1 \frac{(1 + K^{SDS}_{B^+}[D])(1 + K^{SDS}_{Fe(II)}[D])}{(1 + K^{SDS}_{B}[D])(1 + K^{SDS}_{Fe(III)}[D])} \quad (9)$$

obtained, where B and $B^+$ represent $C_nPTZ$ and $C_nPTZ^{\bullet+}$, respectively. The equilibrium data are spectrophotometrically determined and are in reasonable agreement with those estimated by kinetic measurements; they are plotted as a function of surfactant concentration in Figure 6. For $C_{12}PTZ$ the $K^w_1$ for $C_4PTZ$ was assumed. The values for $K^{SDS}_B$ and $K^{SDS}_{B^+}/K^{SDS}_B$ for $C_1PTZ$ have been estimated to be $1.7 \times 10^3$ $M^{-1}$ and 5 at $\mu = 0.10$ M, respectively. Since additional aliphatic carbon atoms will increase the binding constants, it is reasonable to assume that for [SDS] $\geq 1 \times 10^{-2}$ M expression 9 can be modified as follows:

$$\frac{K^{SDS}_{1,exp}}{K^w_1} = \frac{K^{SDS}_{B^+}(1 + K^{SDS}_{Fe(II)}[D])}{K^{SDS}_{B}(1 + K^{SDS}_{Fe(III)}[D])} \quad (10)$$

For $[D] \geq 1 \times 10^{-2}$ M we can assume that $K^{SDS}_{Fe(III)}[D] \gg 1$ (see below), and then eq 10 can be rewritten as

$$\frac{K^{SDS}_{1,exp}}{K^w_1} = \frac{K^{SDS}_{B^+}}{K^{SDS}_{B}K^{SDS}_{Fe(III)}}\left(K^{SDS}_{Fe(II)} + \frac{1}{[D]}\right) \quad (11)$$

Figure 7 shows the equilibrium data plotted according to eq 11. From this equation it follows that the ratio intercept/slope should give $K^{SDS}_{Fe(II)}$; this value is $(1.0 \pm 0.2) \times 10^2$ $M^{-1}$ ($\mu$ = 0.10 M). From the slope, $K^{SDS}_{B^+}/(K^{SDS}_{B}K^{SDS}_{Fe(III)}) = (3.5 \pm 0.5) \times 10^{-3}$ $M^{-1}$ for $C_1PTZ$. Since it was previously determined

$K^{SDS}_{B^+}/K^{SDS}_{B} = 5$ for $C_1PTZ$,[2] it follows that $K^{SDS}_{Fe(III)} = (1.5 \pm 0.3) \times 10^3\ M^{-1}$ ($\mu = 0.10$ M).

The electrostatic contribution to the micellar binding can be estimated from eq 12, where $z$ is the ionic charge and $\phi$ the surface

$$K^{elec} = \exp(-z\phi/25.69) \quad (12)$$

potential of the micelle; in this equation the variation of $\phi$ with the ionic strength is not considered, but at $\mu = 0.10$ M, $\phi$ can be estimated to be -75 to -85 mV[19] and the $Fe^{3+}/Fe^{2+}$ ratio for the electrostatic contribution to the binding constant should be 0.04-0.06, in good agreement with the experimental result; at $\mu = 0.02$ M, if $\phi$ is assumed in the range -100 to -120 mV, the ratio should be 0.01-0.02 (see below). In addition, from eq 11, the ratios of the different intercepts (and slopes) for the different $C_nPTZ$'s give $(K^{SDS}_{B^+}/K^{SDS}_{B})_{C1PTZ}/(K^{SDS}_{B^+}/K^{SDS}_{B})_{C2PTZ,C4PTZ}$. These ratios are ca. 1.2-1.3 for $C_1PTZ$ over $C_2PTZ$ and ca. 1.5-2 for $C_1PTZ$ over $C_4PTZ$.

Although the data are affected by experimental uncertainty, the trend for $K^{SDS}_{B^+}/K^{SDS}_{B}$ is in the order $C_1PTZ > C_2PTZ > C_4PTZ$. This suggests that the contribution of the positive charge to the binding constant is decreasing as the overall hydrophobicity is increasing. This fact seems to be confirmed by the results obtained for $C_{12}PTZ$. At $\mu = 0.10$ M and in the range [SDS] = 0.05-0.20 M, $K^{SDS}_{1,exp} = 0.34 \pm 0.05\ M^{-1}$. If the value of $K^{w}_{1}$ is assumed to be equal to that of $C_4PTZ$ (i.e., 6.5 $M^{-1}$), one obtains $(K^{SDS}_{1,exp}/K^{w}_{1})_{C_{12}PTZ} = 0.05$. Because analogous values for $(K^{SDS}_{Fe(II)}/K^{SDS}_{Fe(III)})$ have been estimated (see above), it follows that $(K^{SDS}_{B^+}/K^{SDS}_{B})_{C_{12}PTZ}$ is ca. 1. This conclusion is not profoundly changed if the value of $K^{w}_{1}$ for $C_{12}PTZ$ is chosen in the range 3-15 (in the most unfavorable case, i.e., $K^{w}_{1} = 3$, $(K^{SDS}_{B^+}/K^{SDS}_{B})_{C_{12}PTZ}$ should be ca. 2).

Measurements at $\mu = 0.02$ M allowed the estimation of $K^{SDS}_{1,exp} = 0.12 \pm 0.03\ M^{-1}$ in the range 0.10-0.15 M SDS. $K^{w}_{1}$ results are slightly depressed at $\mu = 0.02$ M for $C_1PTZ$ (from 2.4 to 1.9);[2] the same is assumed for $C_4PTZ$, and with $K^{SDS}_{Fe(II)}/K^{SDS}_{Fe(III)}$ in the range 0.01-0.02 (see above), it follows again that the ratio $K^{SDS}_{B^+}/K^{SDS}_{B}$ for $C_{12}PTZ$ is close to 1 also at this lower ionic strength.

## Conclusions

In the present study the variation of the hydrophobicity of one reactant and the charge of the micellar aggregates have been shown to greatly affect the location of the reaction and the rate of the electron-transfer process.

An attempt has been devoted to evaluate the contribution of electrostatic and hydrophobic effects and their mutual dependencies. The data can also give some useful informations on the interactions of hydrophobic ions with charged membranes.[22-24]

*Acknowledgment.* Support from Eniricerche and MURST is kindly acknowledged.

(22) Honig, B. H.; Hubbell, W. L.; Flewelling, R. F. *Annu. Rev. Biophys. Biophys. Chem.* **1986**, *15*, 163.
(23) McLaughin, S. *Annu. Rev. Biophys. Biophys. Chem.* **1989**, *18*, 113.
(24) Matsumura, H.; Furusawa, K. *Adv. Colloid Interface Sci.* **1989**, *30*, 71.

# Time-Resolved EPR Studies on the Photochemical Hydrogen Abstraction Reactions and the Excited Triplet States of 4-Substituted Pyridines

**Shozo Tero-Kubota,* Kimio Akiyama, Tadaaki Ikoma, and Yusaku Ikegami**

*Chemical Research Institute of Non-Aqueous Solutions, Tohoku University, Katahira 2-1-1, Sendai 980, Japan* *(Received: May 29, 1990; In Final Form: July 10, 1990)*

Photochemical hydrogen abstraction reactions and the lowest excited triplet states taking part in the initial process have been investigated for several pyridine derivatives by using the time-resolved EPR method. The emissive CIDEP spectrum obtained from the laser photolysis of 4-acetylpyridine (**1**) in 2-propanol was assigned to the corresponding ketyl radical, proving initial hydrogen abstraction by the carbonyl group. In the cases of 4-cyano-(**2**) and 4-methoxycarbonyl-(**3**) pyridines, and 4-pyridinecarboxamide (**4**), enhanced absorptive CIDEP spectra due to the corresponding 1-hydropyridinyl radicals were observed, suggesting the preferential population to the lowest sublevel in the intersystem crossing. The triplet EPR and phosphorescence spectra observed at 77 K indicate that $T_1$ of **1** is mainly the carbonyl $n\pi^*$ state with a small contribution from the $\pi\pi^*$ state. The $T_1$ states of **2**, **3**, and **4** are considered to be of mixed character between the pyridine $^3B_1(n\pi^*)$ and $^3A_1(\pi\pi^*)$ states, though the interaction is smaller than that of unsubstituted pyridine because of raising of the $\pi\pi^*$ state by electron-withdrawing groups. It is proposed that the $T_1$ states of **2**-**4** have smaller deviation from the planar conformation than the $T_1$ state of unsubstituted pyridine.

## Introduction

The time-resolved EPR (TREPR) technique has been successfully employed to elucidate photochemical reaction mechanisms, since the CIDEP spectra observed give information about not only the radical intermediate with a short lifetime but also the character of the excited states taking part in the reaction.[1-6] The method is also a powerful tool to measure short-lived excited triplet states in some matrices at low temperatures.[7,8] Although

(1) Wong, S. K. *J. Am. Chem. Soc.* **1978**, *100*, 5488.
(2) (a) Depew, M. C.; Liu, Z.; Wan, J. K. S. *J. Am. Chem. Soc.* **1983**, *105*, 2480. (b) Depew, M. C.; Wan, J. K. S. *J. Phys. Chem.* **1986**, *90*, 6597.
(3) (a) Akiyama, K.; Tero-Kubota, S.; Ikenoue, T.; Ikegami, Y. *Chem. Lett.* **1984**, 906. (b) Ikegami, Y. *Rev. Chem. Intermed.* **1986**, *7*, 91. (c) Shimoishi, H.; Akiyama, K.; Tero-Kubota, S.; Ikegami, Y. *Chem. Lett.* **1988**, 251.
(4) (a) Yamauchi, S.; Hirota, N. *J. Phys. Chem.* **1984**, *88*, 4631. (b) Tominaga, K.; Yamauchi, S.; Hirota, N. *J. Phys. Chem.* **1988**, *92*, 5160.
(5) (a) Basu, S.; McLauchlan, K. A.; Ritchie, A. J. D. *Chem. Phys.* **1983**, *79*, 95. (b) Buckley, C. D.; McLauchlan, K. A. *Chem. Phys.* **1984**, *86*, 323. (c) Buckley, C. D.; Grant, A. I.; McLauchlan, K. A.; Ritchie, A. J. *Faraday Discuss., Chem. Soc.* **1984**, *78*, 250. (d) Buckley, C. D.; McLauchlan, K. A. *J. Photochem.* **1984**, *27*, 311. (e) Buckley, C. D.; McLauchlan, K. A. *Mol. Phys.* **1985**, *54*, 1.
(6) (a) Sakaguchi, Y.; Hayashi, H.; Murai, H.; I'Haya, J.; Mochida, K. *Chem. Phys. Lett.* **1985**, *120*, 401. (b) Sakaguchi, Y.; Hayashi, H.; Murai, H.; I'Haya, J. *J. Am. Chem. Soc.* **1988**, *110*, 7575.
(7) (a) Tero-Kubota, S.; Migita, K.; Akiyama, K.; Ikegami, Y. *J. Chem. Soc., Chem. Commun.* **1988**, 1067. (b) Akiyama, K.; Ikegami, Y.; Tero-Kubota, S. *J. Am. Chem. Soc.* **1987**, *109*, 2538.
(8) (a) Hirota, N.; Yamauchi, S.; Terazima, M. *Rev. Chem. Intermed.* **1987**, *8*, 189. (b) Yamauchi, S.; Hirota, N. *J. Am. Chem. Soc.* **1988**, *110*, 1346.

0022-3654/91/2095-0766$02.50/0 